AEM Journals.ASM.org

MINIREVIEW

Mapping of Heavy Metal Ion Sorption to Cell-Extracellular Polymeric Substance-Mineral Aggregates by Using Metal-Selective Fluorescent Probes and Confocal Laser Scanning Microscopy

Likai Hao,[a] Jianli Li,[b] Andreas Kappler,[a] Martin Obst[a]

Center for Applied Geoscience, Eberhard Karls University of Tuebingen, Tuebingen, Germany[a]; College of Chemistry and Materials Science, Northwest University, Xi'an, Shaanxi, People's Republic of China[b]

Biofilms, organic matter, iron/aluminum oxides, and clay minerals bind toxic heavy metal ions and control their fate and bioavailability in the environment. The spatial relationship of metal ions to biomacromolecules such as extracellular polymeric substances (EPS) in biofilms with microbial cells and biogenic minerals is complex and occurs at the micro- and submicrometer scale. Here, we review the application of highly selective and sensitive metal fluorescent probes for confocal laser scanning microscopy (CLSM) that were originally developed for use in life sciences and propose their suitability as a powerful tool for mapping heavy metals in environmental biofilms and cell-EPS-mineral aggregates (CEMAs). The benefit of using metal fluorescent dyes in combination with CLSM imaging over other techniques such as electron microscopy is that environmental samples can be analyzed in their natural hydrated state, avoiding artifacts such as aggregation from drying that is necessary for analytical electron microscopy. In this minireview, we present data for a group of sensitive fluorescent probes highly specific for Fe^{3+}, Cu^{2+}, Zn^{2+}, and Hg^{2+}, illustrating the potential of their application in environmental science. We evaluate their application in combination with other fluorescent probes that label constituents of CEMAs such as DNA or polysaccharides and provide selection guidelines for potential combinations of fluorescent probes. Correlation analysis of spatially resolved heavy metal distributions with EPS and biogenic minerals in their natural, hydrated state will further our understanding of the behavior of metals in environmental systems since it allows for identifying bonding sites in complex, heterogeneous systems.

Biofilms are the dominant form of microbial life on Earth (1), and the organic material that is present in biofilms significantly impacts the cycling and sequestration of toxic heavy metals in the environment (2, 3). The underlying sorption and complexation mechanisms are difficult to evaluate (4), since biofilms are highly dynamic and complex structures that consist of diverse biomacromolecules (5) and the *in situ* heavy metal distributions are readily influenced by common invasive analysis approaches such as sequential extractions for the determination of different metal fractions. Here, we introduce a promising approach for studying the distribution and sorption of heavy metals in biofilms and cell-extracellular polymeric substance (EPS)-mineral aggregates (CEMAs) under close-to-natural conditions using confocal laser scanning microscopy (CLSM) in combination with highly selective metal ion-sensitive fluorescence probes. This approach is frequently used for metal detection in cell biology but was rarely applied in environmental and geomicrobiology research due to a former lack of highly selective fluorescence probes and due to the complexity of environmental biofilms and CEMAs.

Biofilms are mainly composed of water, microorganisms, and an EPS matrix (6) that consists of mostly polysaccharides and proteins (7). Environmental biofilms are complex and dynamic structures (5) that can create microscale variations of pH and redox conditions. They often contain mineral particles that can either be trapped by (8, 9) or precipitated within (2, 10) the EPS matrix. Biofilms coat most surfaces of minerals, soil aggregates, and sediments in natural aquatic environments (11, 12). Most importantly, functional groups within biofilms play an essential role in metal cycling in the environment, (13); thus, they can act as a sink for toxic heavy metals (14) from geochemical sources and industrial pollution (15). Both organic compounds such as EPS and bacterial cell surfaces (16) and Fe/Mn oxides (17–20) can serve as sorbents and therefore display a variety of sorption/complexation sites that differ regarding their sorption capacities and properties (8) and ultimately can influence the transport and fate of heavy metals in aquatic environments (21).

One of the key goals in the interdisciplinary approaches used by geochemists, environmental microbiologists, and geomicrobiologists is to understand the mechanisms and to predict the impact of metal-microbe interactions in native biofilms (15). A number of different approaches have been used to investigate the heavy metal distribution and sorption capacity, such as sequential extraction and modeling approaches for the study of biofilms under controlled and reproducible conditions (4). It is, however, difficult to derive insights into mechanisms from studying bulk data that are representative of an average of systems that are heterogeneous at the microscale, and thus, imaging approaches that are able to capture the spatial heterogeneity such as microscopic techniques (4, 7, 22–24) combined with image analysis are promising methods. Such spatially resolved studies have been employed in *in situ* EPS lectin-binding analysis in combination with CLSM, which allowed for the assessment of the glycoconjugate distribu-

Published ahead of print 23 August 2013

Address correspondence to Likai Hao, likai.hao@uni-tuebingen.de.

L.H. and J.L. contributed equally to this work.

Supplemental material for this article may be found at http://dx.doi.org/10.1128/AEM.02454-13.

doi:10.1128/AEM.02454-13

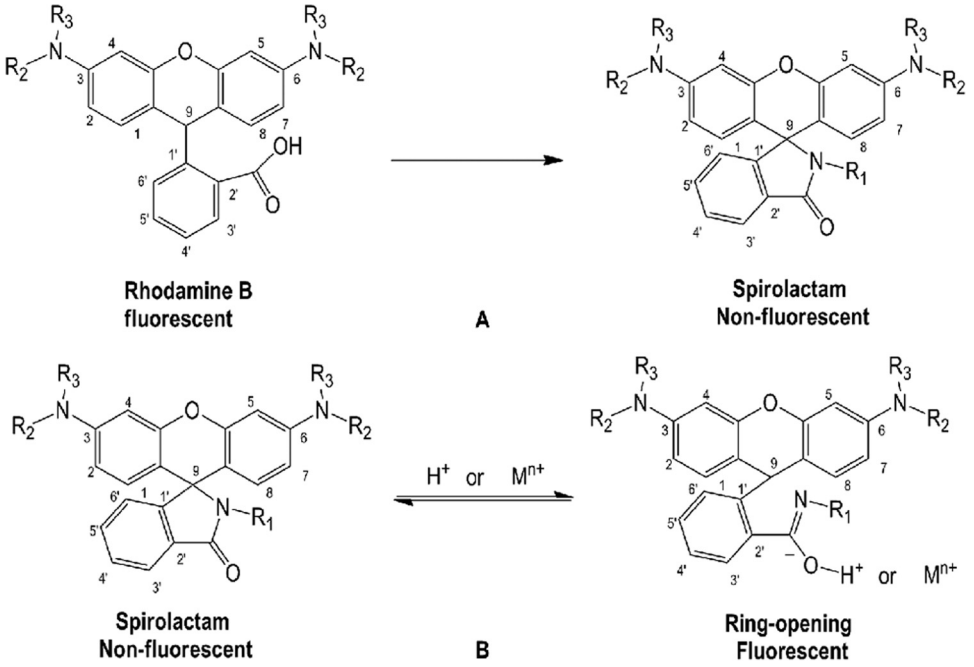

FIG 1 (A) N-, O-, and S-based moieties bound at the R1 position of rhodamine B/6G form a spirolactam ring and create active binding sites for target metal ions and thus switch off the fluorescence of rhodamine B/6G. Modification of the xanthene moiety at the R2 and R3 positions of the amino groups results in improvement of the photophysical properties of these probes. (B) Target metal cation-induced spirolactam ring-opening and/or low pH each triggers the "turn-on" of the fluorescence of rhodamine derivatives.

tion in fully hydrated, native biofilms (25, 26). Another study used CLSM to study associations of Fe(III) minerals and Fe(III) oxyhydroxides with biofilms in Fe^{2+}-rich solutions (27). In the last decade, there have even been a few attempts at using the fluorescent probes Newport Green and Fluozin-1 for the detection of metals in biofilms. Newport Green and Fluozin-1 are well-established metal fluorescent probes with relatively poor selectivity; Newport Green shows different dissociation constants and thus sensitivities to nickel, cadmium, and zinc, while Fluozin-1 shows different dissociation constants for cadmium and zinc since they have different binding sites. Several studies of hydrated biofilms applying dual labeling of bacterial cells and the respective metals have revealed that Ni, Zn, and Cd show reasonably heterogeneous distributions in biofilms (28–30). In all of these studies, bacterial cell walls bound and enriched metal ions due to cellular sorption. These studies concluded that negatively charged functional groups on the cell walls provide binding sites for heavy metals. In additional to the visualization of labeled metals as at the cell surface by CLSM, the authors concluded from bulk measurement that EPS also sequestered heavy metal ions. This, however, was not demonstrated with CLSM data. Newport Green and Fluozin-1 do not allow for an unambiguous detection of specific target metal species due to their poor selectivity and thus have limited applicability for environmental research.

Therefore, to further our mechanistic understanding of metal binding in CEMAs and biofilms, novel approaches for mapping the distribution of metal species, cell surfaces, and EPS that are noninvasive, sensitive, and highly specific for the respective metal species are required (4, 31). More than 1,000 different small organic molecule-based metal fluorescent probes have been described since 1997 that allow for quantitative analysis of dissolved metal concentrations and microscopic metal localization in biological samples in combination with CLSM (32–35). However, this has been applied almost exclusively in the field of cell biology. In this review, we focus on specific metal-induced rhodamine spirolactam ring-opening "turn-on"-type fluorescent probes (32, 35–37); we discuss strategies of how to select a metal-specific fluorescent probe for environmental research such as sorption studies of heavy metals in environmental samples such as biofilms and CEMAs to further our understanding of metal sorption under both anoxic and oxic conditions. Since, to our current knowledge, no environmental or geomicrobiology-related applications of such highly selective metal fluorescent probes were published so far, we performed a case study to ensure the applicability of such probes to heterogeneous samples of bacteriogenic CEMAs. We present data of heavy metal sorption to CEMAs formed by the anaerobic, phototrophic Fe(II)-oxidizing bacterium *Rhodobacter ferrooxidans* strain SW2. The materials and methods for the presented experiment can be found in the supplemental material.

WHAT IS A METAL FLUORESCENT PROBE?

Fluorochromes or fluorophores are compounds that absorb visible or UV light and emit fluorescent light of longer wavelengths (38). To date, various fluorophores have been employed as chemosensors for heavy metal ions (HMs), such as xanthenes, including rhodamines (39) and fluoresceins, which are highly favorable because of excellent photophysical properties (i.e., fluorescence intensity and stability) (40) and their biocompatibility. The modified amino groups of the rhodamine moiety (position 3 and 6), the hydroxyl group of fluorescein, the carboxyphenyl ring (position 4′ and 5′), and the carboxylic acid group (position 2′) create an active binding site for target metal ions (Fig. 1A) (41). Probes

that bind metals noncovalently and reversibly are usually called chemosensors, while probes that bind metals covalently and irreversibly are referred to as chemodosimeters (35). Since the differentiation is not of relevance for studies that are in equilibrium over time scales of the microscopy data acquisition (i.e., a maximum of a few hours), we will not differentiate here between the two classifications but rather use the general phrase "metal fluorescent probe" to encompass both types of probes.

Metal fluorescent probes are designed to be highly selective for specific metal ions, yielding detectable fluorescence signal intensity, and hence sensitivity, into the nanomolar range. Dyes with a bimodal emission spectrum have one emission maximum that is sensitive to the target metal and another maximum that is either not sensitive or inversely sensitive. These two maxima are exploited as ratiometric fluorescent probes and achieve low background fluorescence. In a ratiometric approach, the concentrations are also derived from the intensity ratio of the emission peaks, instead of a single peak. These probes are usually well suited for quantitative mapping. Metal fluorescent probes were originally developed for cell biology applications, which aimed at intracellular metal ion labeling, and should also be useful in mapping extracellular heavy metals in environmental samples and laboratory cultures.

In most cases, the change of the emission response of the metal fluorescent probe is based on a chemical reaction between the reactive center of the probe molecule and the metal cation. Most irreversible metal fluorescent probes are highly selective for a specific metal. We therefore distinguish between probes for which a fluorescence enhancement is observed and those in which a fluorescence decrease (quenching) is observed, in the presence of the metal ion. For the so-called "turn-on" probes, the fluorescence enhancement is often accompanied by an emission wavelength shift, which makes them more suitable for CLSM than "turn-off" probes. Most of the metal fluorescent probes steadily fluoresce on the time scale of hours, which is suitable for multiple-labeling CLSM imaging. In summary, many metal fluorescent probes provide useful characteristics for detecting metal cations in biological and biology-related systems (35).

Many bioessential metal-targeted fluorescent probes (e.g., for Zn^{2+}, Fe^{3+}, Cu^{2+}, Cu^{+}, and Ni^{2+} [33, 41–47]) have been used to explore neuronal metal homeostasis (46, 48) and metal-related physiological processes (38). Probes targeting toxic metals (e.g., for Pb^{2+}, Hg^{2+}, Cd^{2+}, Ag^{+}, Au^{+}, and Pt^{2+} [45, 49, 50]) have been used in cellular toxicity studies. We expect that further improvements in probe design (e.g., pH-dependent dual functional probes [51]) will improve the analytical capabilities of CLSM in biological and environmental applications (52).

MECHANISM FOR FLUORESCENCE ENHANCEMENT DURING PROBE-METAL INTERACTIONS

The activity of metal fluorescent probes, i.e., their fluorescence, can be turned on using various mechanisms such as the binding site/signaling approach, the ring-opening of spirocyclic systems (44, 47), the intramolecular cyclic guanylation of thiourea derivatives (53), mild chemical processes such as ion-induced desulfurization (deselenation) followed by hydrolysis, desulfurization (deiodination) followed by cyclization, deprotection, ester hydrolysis, Schiff-base hydrolysis and hydrazide hydrolysis, photoinduced electron transfer (PET), and intermolecular charge transfer (ICT) (54, 55). However, in most cases, the mechanism of spirocyclization is used to activate or to deactivate fluorescence in real time (33). We therefore explain this ring-opening mechanism in brief.

Rhodamine-based molecules with spirolactam structures as a fluorescence trigger (56) are widely used for metal-selective fluorescent probes owing to their almost ideal fluorescence properties. Modifications of rhodamine (e.g., replacing the nitrogen atoms of the xanthene moiety by a urea group and a trimethyl group [57]) facilitate its linkage to a target molecule (58, 59) and also influence the selectivity toward the target metal ion through electronic or steric hindrance effect (60). Rhodamine spirolactam or spirolacton derivatives are nonfluorescent and colorless, whereas metal-induced ring-opening of the corresponding spirolactam/-lacton at neutral pH and/or ring opening of spirolactam/-lacton at low pH values due to protonation of the carbonyl group both could give rise to strong fluorescence emission and a pink color. N-, O-, and S-based groups at the R1 position of rhodamine provide a specific, active binding site for metal ions (Fig. 1A), which can promote a specific metal cation-induced spirolactam ring-opening (Fig. 1B) (35, 61), even through this process is somewhat dependent on the solvent (40, 44). In most cases, the selectivity of the spirolactam-based probes is sufficient to easily discriminate, e.g., other (bivalent) cations from the target metal ion by several orders of magnitude in terms of fluorescence intensity enhancement (e.g., for Cu^{2+} probe, see Fig. 4 and 6 in reference 62, and for Hg^{2+} probe, see Fig. 10 in reference 63). These metal fluorescent probes are currently not yet commercially available. However, interested researchers can contact the authors for more information.

SELECTION OF A METAL-SELECTIVE "TURN-ON" FLUORESCENT PROBE

The successful mapping of HMs by CLSM requires the selection of a probe with high sensitivity under the experimental conditions. Some parameters to consider during probe selection are the following.

(i) Is the target metal ion located extra- or intracellularly? Many metal ions are essential elements for all living organisms, required for the reactive centers of enzymes, but the required concentrations of these metal ions are generally quite low (i.e., nanomolar levels) (64, 65). As a result, intracellular HM concentrations might still be in the nanomolar range even if concentrations in the extracellular environment are higher by many orders of magnitude.

(ii) What are the E_h/pH conditions of the experiment? The pH, ionic composition, and redox state of intracellular versus extracellular environments may differ due to cells generating microgradients that facilitate uptake of nutrients or enhance metabolic energy efficiency (i.e., a proton pump). The effect of pH on metal solubility is difficult to distinguish from other autocorrelated parameters such as the protonation of sorption sites and the binding properties of the fluorescent probe. Thus, it is important to verify that the probe covers the respective concentration range of the HM species of interest, under the conditions that occur within the sample. Since it has the most influence on chemical speciation (66), pH can diminish the sensitivity of a particular fluorescent probe. Besides pH, the speciation of HMs can be controlled by the redox conditions in the sample. Thus, it might be necessary to identify the redox conditions and quantify the abundance of all relevant HM species under the pH/redox conditions observed in

the sample (e.g., by thermodynamic modeling approaches or E_h measurements) (67, 68).

(iii) What is the concentration of the target metal ion? Dissolved concentrations of most essential target metal ions in microbial culture medium range from 10 to 800 nM (64, 65), whereas concentrations found in the environment can vary by many orders of magnitude. The fluorescent probe might not be sensitive to all metal species in a single sample (e.g., metal ions sorbed to mineral surfaces or complexed by organics), which should be verified in separate control experiments with the target metal ion and the mineral and the target ion and the organics when interpreting the measured distribution pattern. Often, metal ions are enriched within microenvironments due to sorption or complexation. The enrichment factors depend on the surface properties and functional groups of the organic sorbent. Some metal species preferentially bind to functional groups of organic matter, whereas others are preferentially sorbed to/coprecipitated with mineral phases.

(iv) How sensitive is the target metal ion to fluorescent probe disturbance? The addition of the fluorescent probe may alter the distribution, mobility, and bioavailability and thus the function of the target metal ions. Potential effects depend on the probe's solubility, which affects the upper limit of the detection range, and the dissociation constant of the dye-metal complex, which might reduce metal availability more or less strongly for higher or lower constants, respectively. Additional artifacts of fluorescence staining might be caused by interactions of the fluorescent probe with the cells, i.e., biotoxicity effects, or from inhomogeneous distribution of the probe in heterogeneous samples; the latter can be overcome by using ratiometric probes.

(v) What type of probe will be used? For qualitative and (semi-) quantitative HM mapping, almost all highly metal-selective and -sensitive, rhodamine-based "turn-on" fluorescent probes can be utilized for CLSM imaging. For quantitative mapping, ratiometric probes which can minimize background fluorescence are preferred (69) due to their higher precision and selectivity and lower interference with other nontarget metals.

The selected fluorescent probe should have the necessary sensitivity, and the resulting fluorescence signal should be stable. The fluorescent probe should clearly discriminate the target metal species from other metal species that are present in the system (29). In particular, for environmental studies where solutions can contain multiple ions at significantly different concentration ranges, a lack of the required selectivity has been a major disadvantage of many conventional and commercially available metal fluorescent probes. Additionally, the selected fluorescent probe should have a strong fluorescence enhancement within a few minutes, essential for multiple labeling or time-lapse CLSM. The fluorescent probe should not be saturated at the concentration of the target metal present in the sample. Furthermore, the probe should function at a broad concentration range for metal semiquantitative detection with good linearity. The fluorescent probe should be water soluble, should have a low toxicity to cell metabolism, and should be environmentally friendly. Finally, depending on the available CLSM instrumentation, often visible-light excitation and emission are preferred since instruments in this wavelength range are readily available. The basic principles of selection criteria for fluorescent probes were described efficiently by Czarnik in 1998: "'meets all the demands of the application'—no more, no less" (70).

SPECIFIC METAL FLUORESCENT PROBES

In the following, we summarize relevant examples that illustrate the performance of selected metal fluorescent probes (Fe^{3+}, Cu^{2+}, Zn^{2+}, and Hg^{2+}) for environmental samples, their different sorption properties, and their different toxicities. Almost all metal fluorescent probes discussed here in detail can be used in combination with a "basic" CLSM equipped with multiple lasers.

Fe^{3+} fluorescent probes. Iron is a redox-active, bioessential metal. The majority of intracellular biologically bound iron is tightly bound by enzymes (48). We selected four Fe^{3+} fluorescent probes from more than 100 recently reported articles (Table 1) based on the criteria described above. Their excitation and emission spectrum is almost always based on a rhodamine B backbone, which is readily excited with commonly available lasers. The emission peaks are around 570 to 595 nm, so these probes combine well with other commercially available fluorescent dyes that bind to DNA (such as Syto dyes) and polysaccharides (such as lectin-Alexa Fluor conjugates), i.e., they have nonoverlapping emission maxima. Using multiple dyes for these sample components facilitates correlation analysis, e.g., the colocalization of Fe^{3+} ions to microbial cells and/or EPS. In addition, all of these selected Fe^{3+} fluorescent probes show a high selectivity and result in no significant background fluorescence with other, mono- or bivalent cations. Thus, they can be used in solutions such as culture media for environmentally relevant bacteria, which contain many metals (e.g., Na^+, K^+, Ca^{2+}, Cd^{2+}, Mg^{2+}, Co^{2+}, Mn^{2+}, Zn^{2+}, Ni^{2+}, Hg^{2+}, Cu^{2+}, and Fe^{2+}). All of these probes are sensitive to micromolar Fe^{3+} levels (detection range, 1 to 100 μM), and some show an excellent linearity within certain concentration ranges. In addition, all of these probes show a "turn-on" response to Fe^{3+} and are therefore easier to use in a (semi-)quantitative way.

Cu^{2+} fluorescent probes. Copper is an essential element for all living organisms, but it is toxic when micromolar levels are exceeded (48). More than 220 Cu^{2+} fluorescent probes have been reported during the last 15 years. The design of the first Cu^{2+} fluorescent probe was reported in 1997 (71, 72), and it was also the first reported metal fluorescent probe. Most Cu^{2+} probes show excitation and emission characteristics similar to those of Fe^{3+} probes, and their detection ranges vary from 0.002 μM to 60 μM Cu^{2+}. All of the selected Cu^{2+} fluorescent probes show high selectivity over other essential metals such as Na^+, K^+, Ca^{2+}, Cd^{2+}, Mg^{2+}, Co^{2+}, Mn^{2+}, Zn^{2+}, Ni^{2+}, Hg^{2+}, Cu^{2+}, and Fe^{2+}. Probes 1 and 2 (Table 1) show different spectral properties compared to most Fe^{3+} fluorescent probes, with emission peaks between 540 and 560 nm. This spectral range not only allows their use in combination with other dyes to analyze the correlation of Cu^{2+} with cells and EPS but also provides the possibility of multimetal labeling in combination with other metal-sensitive probes such as Fe^{3+} probes to analyze the correlation of Cu^{2+} with Fe^{3+}.

Zn^{2+} fluorescent probes. Similar to iron and copper, zinc is also an essential nutrient to all forms of life and exists mostly in its divalent form within biological environments (48). We screened 200 Zn^{2+} probes and selected 4 candidates for environmental research. Probes 1 and 4 (Table 1) are excited with visible laser wavelengths and displayed emission maxima around 570 to 590 nm, whereas probe 3 emits maximally at 510 to 520 nm. The latter again can be used, e.g., in combination with Fe^{3+} probes. The ratiometric probe 2 can be used for subquantitative and quantitative mapping.

TABLE 1 Summary of specific metal fluorescent probes[a]

Target and probe no.	Chemical structure	Ex (nm)	Em (nm)	DL (μM)	DR (μM)	Solvent	Reference
Fe^{3+}							
1	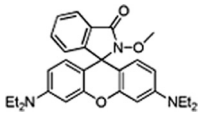	530	580	1	0–20	MeOH	88
2	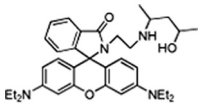	561	583	0.11	1–100	Tris-HCl	89
3	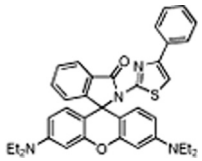	558	580	5	5–20	MeOH	90
4	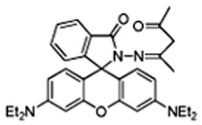	570	593	0.004	0.5–50	Tris-HCl	91
Cu^{2+}							
1	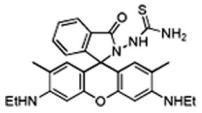	480	554	0.002	0–0.005	CH_3CN	92
2	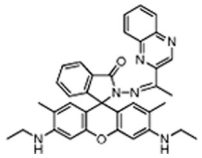	520	545	0.04	0.5–1	PBS	93
3	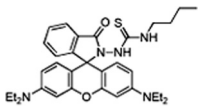	510	580	0.16	0.08–2.5	CH_3CN	62
4	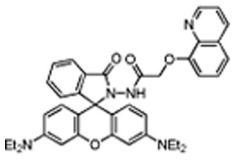	555	587	0.005	0–60	CH_3CN	94
Zn^{2+}							
1	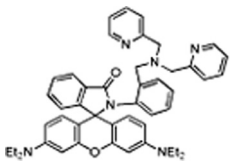	550	595		0–1,800	PIPES	95

(Continued on following page)

TABLE 1 (Continued)

Target and probe no.	Chemical structure	Ex (nm)	Em (nm)	DL (μM)	DR (μM)	Solvent	Reference
2	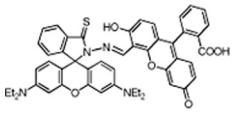	485	518, 590	0.04	0.2–20	CH_3CN	56
3	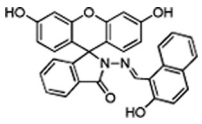	398	513	0.1	0–2	MeOH	96
4	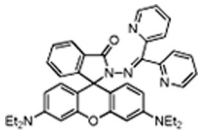	530	581		0.2–50	EtOH	97
Hg^{2+}							
1	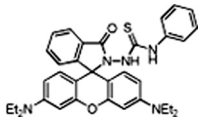	450	537	0.004	0.004–0.05	Water	98
2	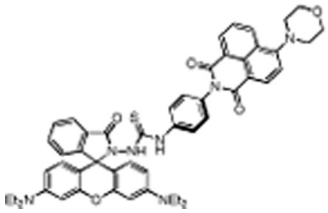	400	545, 585	0.03	0.03–1	MeOH	99
3	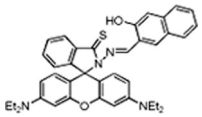	510	594	0.0059	0–50	CH_3CN	100
4	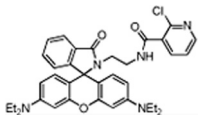	520	582	0.008	0–10	MeOH	63

[a] Abbreviations: Ex, excitation; Em, emission; DL, detection limitation; DR, detection range; CH_3CN, acetonitrile; MeOH, methanol; EtOH, ethanol; PBS, phosphate-buffered saline; PIPES, piperazine-*N*,*N*′-bis(2-ethanesulfonic acid).

The detection ranges of the Zn^{2+} probes vary from submicromolar concentrations to 50 μM. The Zn^{2+} probes are quite selective and only little affected by the presence of additional metal ions.

Hg^{2+} fluorescent probes. Compared to Fe^{3+}, Cu^{2+}, and Zn^{2+}, the Hg^{2+} ion is one of the most critical environmental contaminants because of its extreme toxicity. Mercury is a persistent contaminant, which bioaccumulates in ecosystems (73). Four Hg^{2+} probes were selected for illustrating the possibility for Hg^{2+} mapping. Although reported Hg^{2+} probes have been reviewed before (35, 73), these reviews did not focus on environmental applications. Probes 3 and 4 are excited with common solid-state or gas lasers in the visible light range and emit around 570 to 590 nm (Table 1). Again, this makes them suitable for combining with other fluorochromes to analyze correlations of Hg^{2+} to cellular components and EPS. Probe 1 shows an emission peak at 537 nm and can be combined with Fe^{3+} probes to analyze the correlation of Hg^{2+} with Fe^{3+}. Additionally, the ratiometric probe 2 can be used for subquantitative and quantitative mapping. The relatively high selectivity mitigates interference from additional ions.

APPLICATIONS

In contrast to scanning electron microscopy (SEM) or transmission electron microscopy (TEM), where even the most careful specimen preparation cannot prevent artifacts (74, 75), CLSM and scanning transmission X-ray microscopy (STXM) are powerful tools for *in situ* quantitative or semiquantitative analysis of

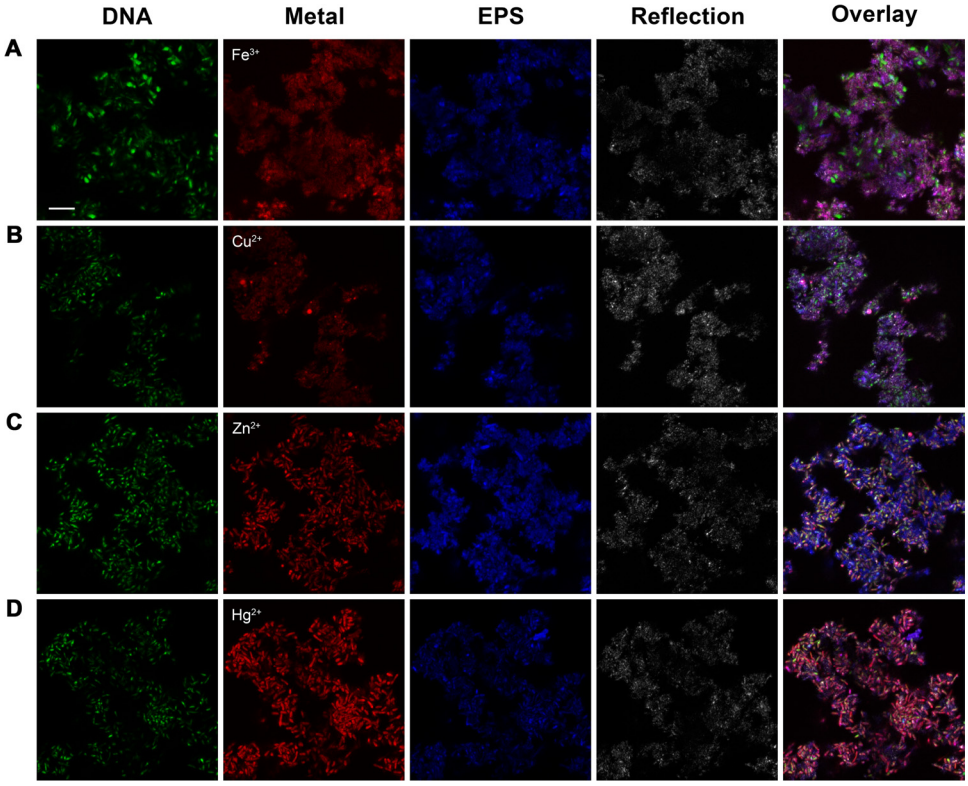

FIG 2 Maximum-intensity projections of multiple channels of 3D data sets from CLSM illustrating the applicability of highly selective metal fluorescent probes for environmental research. For details of the experimental approach, see the supplemental material. The individual false colors illustrate the submicrometer-scale composition of cell-EPS-mineral aggregates formed by the anaerobic, phototrophic Fe(II)-oxidizing bacterium *Rhodobacter ferrooxidans* strain SW2. Four cultures were analyzed, containing no heavy metals (A), Cu^{2+} (B), Zn^{2+} (C), and Hg^{2+} (D). Cells were stained with three probes: SYTO 9 green fluorescent nucleic acid stain (column 1), a probe labeling either Fe^{3+} or the respective heavy metal ion added at 1 μM to the culture (column 2), and the wheat germ agglutinin-Alexa Fluor 633 conjugate labeling EPS (column 3). Fe(III) minerals and Fe(III) oxyhydroxides are visualized by their reflection signal (Ref) (column 4). The overlay of all four signals is shown in column 5. Brighter color indicates a higher metal concentrations. Bar, 5 μm.

environmental samples such as biofilms in their hydrated state (24, 76, 77). These techniques yield reliable information on biofilm structure (78, 79), chemical composition (24, 80), and heavy metal adsorption (24, 28). Moreover, CLSM can be used to explore dynamic microbial population change (24, 81) and mass transport in biofilm systems (78). Another advantage of CLSM over STXM is the accessibility.

Since no examples for the application of these highly selective, metal-specific fluorescent probes in environmental sciences have been published, in this review, we demonstrate the application of the above-described probes to study and to visualize metal distributions in CEMAs formed by Fe(II)-oxidizing bacteria. We are particularly interested in the influence of microbial Fe(II) oxidation on the distribution and fate of Fe^{3+}, Cu^{2+}, Zn^{2+}, and Hg^{2+} in these samples. The distribution and fate of HMs can be influenced by the stress response of the bacteria to toxic metal concentrations, resulting, e.g., in an enhanced production of EPS as a protection mechanism (82, 83). The metals are redox sensitive, and their distribution might be different between their natural hydrated state and dry samples. Thus, CLSM is one of very few suitable techniques that allow for mapping the metals in their natural, hydrated, and anoxic state.

A case study: Fe(II)-oxidizing bacterial-mineral aggregates. In the example, we sought to determine the HM distribution patterns between bacterial cells, EPS, and mineral phases in CEMAs formed by Fe(II)-oxidizing bacteria under anoxic conditions. Figure 2 shows the results of a fluorescent probe-based multilabel CLSM approach that we used to visualize and measure the distribution of metal ion cells and EPS in CEMAs formed by the anaerobic phototrophic Fe(II)-oxidizing bacterium *Rhodobacter ferrooxidans* strain SW2 (84).

The individually added toxic metal ions (i.e., Cu^{2+}, Zn^{2+}, Cd^{2+}, and Hg^{2+}) were each found to be mostly enriched in the EPS-rich matrix of the CEMAs. Fe^{3+} ions were complexed and sorbed by functional groups on the cells' surfaces and within the EPS that derived from microbial Fe(II) oxidation. The local correlation between sorbed Fe^{3+} and other heavy metal ions thus indicates a potential competition of a fraction of the sorption sites in the EPS between Fe^{3+} and the other metal ions, whereas other sites in the EPS seemed to preferentially bind one of the metal ions over the other. In principle, Fe(III) minerals and Fe(III) oxyhydroxides can provide additional binding sites for metal ions, but most likely steric effects in combination with low concentrations of Fe(III) minerals and Fe(III) oxyhydroxide surface-bound metal ions result in no significant fluorescence increase in the case of Fe(III) minerals and Fe(III) oxyhydroxide-bound metals.

CONCLUSION AND OUTLOOK

Reliable multicolor labeling CLSM approaches are currently under development, including combinations such as DNA/protein-

Me^{+}-EPS, or different metal ion multiple labeling, i.e., Fe^{3+}-Cu^{2+}/Zn^{2+}/Ni^{2+}/Cd^{2+}/Hg^{2+}. To confirm the distribution patterns observed by CLSM, it will be necessary to compare the results with distribution patterns obtained by other conventional methods such as scanning electron microscopy (SEM)/transmission electron microscopy (TEM) in combination with energy-dispersive X-ray spectroscopy (EDX), or with STXM, which also allows for analyzing hydrated samples. Further developments and testing are required in particular for tracking microbial Fe(II) oxidation. The success of this approach is heavily dependent on the design and development of highly sensitive and selective Fe^{2+} and Fe^{3+} fluorescent probes that can be synthesized more efficiently. In particular, the Fe^{2+} fluorescent probe design is still a great challenge, and due to the difficult chemical synthesis, only a few probes have been reported so far (85, 86). However, dual-functional iron fluorescent probes, which can be used for Fe^{2+} and Fe^{3+} in combination with chemical agents such as H_2O_2 (87), or depending on pH, have been successfully applied in biological sample imaging (51). More sophisticated approaches such as mapping several metals simultaneously, studying adsorption/desorption processes, simultaneously detecting dynamic changes of intracellular/extracellular and extracellular metals, and the correlative analysis of metal-cell/metal-EPS systems, all depend on further high-quality, purpose-oriented fluorescent probe development.

In summary, the development of CLSM-compatible metal fluorescent probes for use in three-dimensional (3D) and quantitative analytical microscopy is a great challenge to both microscopists and chemists, which demands further discussion, exchange, and extensive collaboration between these two fields. The advantage of being able to analyze samples in their natural hydrated state with a readily available microscopy approach, however, will be a driving force that helps to create new methods for studying the fate of heavy metals in the environment. Spatially resolved correlation analysis and the combination of the multilabeling CLSM approach with other analytical microscopy techniques such as STXM might help to better characterize or even identify the sorption sites with general or specific binding characteristics, respectively. Since the spatial resolution in conventional CLSM is limited in comparison to other approaches, such as electron microscopy, applications of super-high-resolution optical microscopy techniques such as structured illumination microscopy might help to overcome these limitations if metal fluorescent probes that are compatible with these techniques can be developed.

ACKNOWLEDGMENTS

We thank E. D. Swanner, J. Byrne, Z. Yang, F. Zeitvogel, X. Jin, P. Ingino, G. Schmid, E. Struve, W. Wu, and the geomicrobiology group in Tuebingen for their support. We also thank Z. Zeng (LZU), F. Li (FDU), Y. Xu (ECUST), and J. Liu (Heliosense) for providing high-quality metal probes.

This project was funded by the DFG Emmy-Noether program to M.O. (OB 362/1-1) and the NSF of China (grants 20972124, 21103137, and 21272184).

REFERENCES

1. **Ivleva NP, Wagner M, Horn H, Niessner R, Haisch C.** 2008. In situ surface-enhanced Raman scattering analysis of biofilm. Anal. Chem. **80:** 8538–8544.
2. **Beveridge TJ, Makin SA, Kadurugamuwa JL, Li Z.** 1997. Interactions between biofilms and the environment. FEMS Microbiol. Rev. **20:**291–303.
3. **Sabater S, Guasch H, Ricart M, Romaní A, Vidal G, Klünder C, Schmitt-Jansen M.** 2007. Monitoring the effect of chemicals on biological communities. The biofilm as an interface. Anal. Bioanal. Chem. **387:** 1425–1434.
4. **van Hullebusch ED, Zandvoort MH, Lens PNL.** 2003. Metal immobilisation by biofilms: mechanisms and analytical tools. Rev. Environ. Sci. Biotechnol. (NY) **2:**9–33.
5. **Pavithra D, Doble M.** 2008. Biofilm formation, bacterial adhesion and host response on polymeric implants—issues and prevention. Biomed. Mater. **3:**034003. doi:10.1088/1748-6041/3/3/034003.
6. **Yang L, Hu Y, Liu Y, Zhang J, Ulstrup J, Molin S.** 2011. Distinct roles of extracellular polymeric substances in *Pseudomonas aeruginosa* biofilm development. Environ. Microbiol. **13:**1705–1717.
7. **Pamp SJ, Sternberg C, Tolker-Nielsen T.** 2009. Insight into the microbial multicellular lifestyle via flow-cell technology and confocal microscopy. Cytometry A **75:**90–103.
8. **Flemming H-C.** 1995. Sorption sites in biofilms. Water Sci. Technol. **32:**27–33.
9. **Flemming H-C, Leis A.** 2003. Sorption properties of biofilms. Encyclopedia of environmental microbiology. John Wiley & Sons, Inc., New York, NY. doi:10.1002/0471263397.
10. **Petrash DA, Lalonde SV, Raudsepp M, Konhauser KO.** 2011. Assessing the importance of organic matrix materials in biofilm chemical reactivity: insights from proton and cadmium adsorption onto the commercially available biopolymer alginate. Geomicrobiol. J. **28:**266–273.
11. **Gorbushina AA.** 2007. Life on the rocks. Environ. Microbiol. **9:**1613–1631.
12. **Lünsdorf H, Erb RW, Abraham WR, Timmis KN.** 2000. 'Clay hutches': a novel interaction between bacteria and clay minerals. Environ. Microbiol. **2:**161–168.
13. **Toner B, Manceau A, Marcus MA, Millet DB, Sposito G.** 2005. Zinc sorption by a bacterial biofilm. Environ. Sci. Technol. **39:**8288–8294.
14. **Späth R, Flemming HC, Wuertz S.** 1998. Sorption properties of biofilms. Water Sci. Technol. **37:**207–210.
15. **Yang S, Ngwenya BT, Butler IB, Kurlanda H, Elphick SC.** 2013. Coupled interactions between metals and bacterial biofilms in porous media: implications for biofilm stability, fluid flow and metal transport. Chem. Geol. **337-338:**20–29.
16. **McLean RJC, Fortin D, Brown DA.** 1996. Microbial metal-binding mechanisms and their relation to nuclear waste disposal. Can. J. Microbiol. **42:**392–400.
17. **Anderson CR, Pedersen K.** 2003. *In situ* growth of *Gallionella* biofilms and partitioning of lanthanides and actinides between biological material and ferric oxyhydroxides. Geobiology **1:**169–178.
18. **Ferris FG, Hallberg RO, Lyvén B, Pedersen K.** 2000. Retention of strontium, cesium, lead and uranium by bacterial iron oxides from a subterranean environment. Appl. Geochem. **15:**1035–1042.
19. **Fru EC, Piccinelli P, Fortin D.** 2012. Insights into the global microbial community structure associated with iron oxyhydroxide minerals deposited in the aerobic biogeosphere. Geomicrobiol. J. **29:**587–610.
20. **Toner B, Manceau A, Webb SM, Sposito G.** 2006. Zinc sorption to biogenic hexagonal-birnessite particles within a hydrated bacterial biofilm. Geochim. Cosmochim. Acta **70:**27–43.
21. **Nelson YM, Lo W, Lion LW, Shuler ML, Ghiorse WC.** 1995. Lead distribution in a simulated aquatic environment: effects of bacterial biofilms and iron oxide. Water Res. **29:**1934–1944.
22. **Denkhaus E, Meisen S, Telgheder U, Wingender J.** 2007. Chemical and physical methods for characterisation of biofilms. Microchim. Acta **158:** 1–27.
23. **Halan B, Buehler K, Schmid A.** 2012. Biofilms as living catalysts in continuous chemical syntheses. Trends Biotechnol. **30:**453–465.
24. **Neu TR, Manz B, Volke F, Dynes JJ, Hitchcock AP, Lawrence JR.** 2010. Advanced imaging techniques for assessment of structure, composition and function in biofilm systems. FEMS Microbiol. Ecol. **72:**1–21.
25. **Neu TR, Lawrence JR.** 1999. Lectin-binding analysis in biofilm systems. Methods Enzymol. **310:**145–152.
26. **Zippel B, Neu TR.** 2011. Characterization of glycoconjugates of extracellular polymeric substances in tufa-associated biofilms by using fluorescence lectin-binding analysis. Appl. Environ. Microbiol. **77:**505–516.
27. **Brydie JR, Wogelius RA, Boult S, Merrifield CM, Vaughan DJ.** 2009. Model system studies of the influence of bacterial biofilm formation on mineral surface reactivity. Biofouling **25:**463–472.
28. **Ueshima M, Ginn BR, Haack EA, Szymanowski JES, Fein JB.** 2008. Cd

adsorption onto *Pseudomonas putida* in the presence and absence of extracellular polymeric substances. Geochim. Cosmochim. Acta **72:** 5885–5895.
29. **Wuertz S, Muller E, Spaeth R, Pfleiderer P, Flemming HC.** 2000. Detection of heavy metals in bacterial biofilms and microbial flocs with the fluorescent complexing agent Newport Green. J. Ind. Microbiol. Biotechnol. **24:**116–123.
30. **Wuertz S, Spaeth R, Hinderberger A, Griebe T, Flemming HC, Wilderer PA.** 2001. A new method for extraction of extracellular polymeric substances from biofilms and activated sludge suitable for direct quantification of sorbed metals. Water Sci. Technol. **43**(6)**:**25–31.
31. **Arnold T, Grossmann K, Baumann N.** 2010. Uranium speciation in biofilms studied by laser fluorescence techniques. Anal. Bioanal. Chem. **396:**1641–1653.
32. **Dean KM, Qin Y, Palmer AE.** 2012. Visualizing metal ions in cells: an overview of analytical techniques, approaches, and probes. Biochim. Biophys. Acta **1823:**1406–1415.
33. **Nagano T.** 2010. Development of fluorescent probes for bioimaging applications. Proc. Jpn. Acad. Ser. B **86:**837–847.
34. **Qian X, Xiao Y, Xu Y, Guo X, Qian J, Zhu W.** 2010. "Alive" dyes as fluorescent sensors: fluorophore, mechanism, receptor and images in living cells. Chem. Commun. **46:**6418–6436.
35. **Yang Y, Zhao Q, Feng W, Li F.** 2013. Luminescent chemodosimeters for bioimaging. Chem. Rev. **113:**192–270.
36. **Li N, Liu ML, Yin WT, Yang Z, Li JL, Shi Z.** 2011. Recent progress in rhodamine-based "OFF-ON" fluorescent probes. Chin. J. Org. Chem. **31:**39–53.
37. **Sun W, Hu DY, Wu ZB, Song BA, Yang S.** 2011. Research progress of fluorescent molecular probes for heavy and transition metallic cations based on rhodamine fluorophore. Chin. J. Org. Chem. **31:**997–1010.
38. **Drummen G.** 2012. Fluorescent probes and fluorescence (microscopy) techniques—illuminating biological and biomedical research. Molecules **17:**14067–14090.
39. **Gonçalves MST.** 2009. Fluorescent labeling of biomolecules with organic probes. Chem. Rev. **109:**190–212.
40. **Chen X, Pradhan T, Wang F, Kim JS, Yoon J.** 2012. Fluorescent chemosensors based on spiroring-opening of xanthenes and related derivatives. Chem. Rev. **112:**1910–1956.
41. **Beija M, Afonso CAM, Martinho JMG.** 2009. Synthesis and applications of rhodamine derivatives as fluorescent probes. Chem. Soc. Rev. **38:**2410–2433.
42. **Kang MY, Lim CS, Kim HS, Seo EW, Kim HM, Kwon O, Cho BR.** 2012. Detection of nickel in fish organs with a two-photon fluorescent probe. Chemistry **18:**1953–1960.
43. **Kikuchi K.** 2010. Design, synthesis and biological application of chemical probes for bio-imaging. Chem. Soc. Rev. **39:**2048–2053.
44. **Kim HN, Lee MH, Kim HJ, Kim JS, Yoon J.** 2008. A new trend in rhodamine-based chemosensors: application of spirolactam ring-opening to sensing ions. Chem. Soc. Rev. **37:**1465–1472.
45. **Kim HN, Ren WX, Kim JS, Yoon J.** 2012. Fluorescent and colorimetric sensors for detection of lead, cadmium, and mercury ions. Chem. Soc. Rev. **41:**3210–3244.
46. **Que EL, Domaille DW, Chang CJ.** 2008. Metals in neurobiology: probing their chemistry and biology with molecular imaging. Chem. Rev. **108:**1517–1549.
47. **Sahoo SK, Sharma D, Bera RK, Crisponi G, Callan JF.** 2012. Iron(III) selective molecular and supramolecular fluorescent probes. Chem. Soc. Rev. **41:**7195–7227.
48. **Domaille DW, Que EL, Chang CJ.** 2008. Synthetic fluorescent sensors for studying the cell biology of metals. Nat. Chem. Biol. **4:**168–175.
49. **Zhang JF, Zhou Y, Yoon J, Kim JS.** 2011. Recent progress in fluorescent and colorimetric chemosensors for detection of precious metal ions (silver, gold and platinum ions). Chem. Soc. Rev. **40:**3416–3429.
50. **Zhang X, Xiao Y, Qian X.** 2008. A ratiometric fluorescent probe based on FRET for imaging Hg^{2+} ions in living cells. Angew. Chem. Int. Ed. **47:**8025–8029.
51. **Sen S, Sarkar S, Chattopadhyay B, Moirangthem A, Basu A, Dhara K, Chattopadhyay P.** 2012. A ratiometric fluorescent chemosensor for iron: discrimination of Fe^{2+} and Fe^{3+} and living cell application. Analyst **137:** 3335–3342.
52. **Yuste R.** 2005. Fluorescence microscopy today. Nat. Methods **2:**902–904.
53. **Duong TQ, Kim JS.** 2010. Fluoro- and chromogenic chemodosimeters for heavy metal ion detection in solution and biospecimens. Chem. Rev. **110:**6280–6301.
54. **Chan J, Dodani SC, Chang CJ.** 2012. Reaction-based small-molecule fluorescent probes for chemoselective bioimaging. Nat. Chem. **4:**973–984.
55. **Xu Z, Yoon J, Spring DR.** 2010. Fluorescent chemosensors for Zn^{2+}. Chem. Soc. Rev. **39:**1996–2006.
56. **Han Z-X, Zhang X-B, Zhuo L, Gong Y-J, Wu X-Y, Zhen J, He C-M, Jian L-X, Jing Z, Shen G-L, Yu R-Q.** 2010. Efficient fluorescence resonance energy transfer-based ratiometric fluorescent cellular imaging probe for Zn^{2+} using a rhodamine spirolactam as a trigger. Anal. Chem. **82:**3108–3113.
57. **Lavis LD, Chao T-Y, Raines RT.** 2006. Fluorogenic label for biomolecular imaging. ACS Chem. Biol. **1:**252–260.
58. **Lavis LD, Raines RT.** 2008. Bright ideas for chemical biology. ACS Chem. Biol. **3:**142–155.
59. **Wysocki LM, Lavis LD.** 2011. Advances in the chemistry of small molecule fluorescent probes. Curr. Opin. Chem. Biol. **15:**752–759.
60. **Sasaki H, Hanaoka K, Urano Y, Terai T, Nagano T.** 2011. Design and synthesis of a novel fluorescence probe for Zn^{2+} based on the spirolactam ring-opening process of rhodamine derivatives. Bioorg. Med. Chem. **19:**1072–1078.
61. **Fölling J, Belov V, Kunetsky R, Medda R, Schönle A, Egner A, Eggeling C, Bossi M, Hell SW.** 2007. Photochromic rhodamines provide nanoscopy with optical sectioning. Angew. Chem. Int. Ed. **46:**6266–6270.
62. **Yu M, Shi M, Chen Z, Li F, Li X, Gao Y, Xu J, Yang H, Zhou Z, Yi T, Huang C.** 2008. Highly sensitive and fast responsive fluorescence turn-on chemodosimeter for Cu^{2+} and its application in live cell imaging. Chemistry **14:**6892–6900.
63. **Yan F, Cao D, Yang N, Yu Q, Wang M, Chen L.** 2012. A selective turn-on fluorescent chemosensor based on rhodamine for Hg^{2+} and its application in live cell imaging. Sens. Actuators B Chem. **162:**313–320.
64. **Posth NR, Huelin S, Konhauser KO, Kappler A.** 2010. Size, density and composition of cell-mineral aggregates formed during anoxygenic phototrophic Fe(II) oxidation: impact on modern and ancient environments. Geochim. Cosmochim. Acta **74:**3476–3493.
65. **Widdel F, Schnell S, Heising S, Ehrenreich A, Assmus B, Schink B.** 1993. Ferrous iron oxidation by anoxygenic phototrophic bacteria. Nature **362:**834–836.
66. **Sauvé S, Hendershot W, Allen HE.** 2000. Solid-solution partitioning of metals in contaminated soils: dependence on pH, total metal burden, and organic matter. Environ. Sci. Technol. **34:**1125–1131.
67. **Hunter RC, Beveridge TJ.** 2010. Metal-bacteria interactions at both the planktonic cell and biofilm levels, p 127–165. *In* Sigel A, Sigel H, Sigel RKO (ed), Biomineralization: from nature to application. John Wiley & Sons, Ltd., Chichester, United Kingdom.
68. **Schröder TJ.** 2005. Solid-solution partitioning of heavy metals in floodplain soils of the rivers Rhine and Meuse: field sampling and geochemical modelling. Wageningen Universiteit, Wageningen, Netherlands.
69. **Tsien RY, Poenie M.** 1986. Fluorescence ratio imaging: a new window into intracellular ionic signaling. Trends Biochem. Sci. **11:**450–455.
70. **Czarnik AW.** 1998. A sense for landmines. Nature **394:**417–418.
71. **Dujols V, Ford F, Czarnik AW.** 1997. A long-wavelength fluorescent chemodosimeter selective for Cu(II) ion in water. J. Am. Chem. Soc. **119:**7386–7387.
72. **Kramer R.** 1998. Fluorescent chemosensors for Cu^{2+} ions: fast, selective, and highly sensitive. Angew. Chem. Int. Ed. **37:**772–773.
73. **El-Safty SA, Shenashen MA.** 2012. Mercury-ion optical sensors. Trends Anal. Chem. **38:**98–115.
74. **Chang HT, Rittmann BE.** 1986. Biofilm loss during sample preparation for scanning electron microscopy. Water Res. **20:**1451–1456.
75. **Schädler S, Burkhardt C, Kappler A.** 2008. Evaluation of electron microscopic sample preparation methods and imaging techniques for characterization of cell-mineral aggregates. Geomicrobiol. J. **25:**228–239.
76. **Hitchcock AP, Dynes JJ, Lawrence JR, Obst M, Swerhone GD, Korber DR, Leppard GG.** 2009. Soft X-ray spectromicroscopy of nickel sorption in a natural river biofilm. Geobiology **7:**432–453.
77. **Xavier JB, White DC, Almeida JS.** 2003. Automated biofilm morphology quantification from confocal laser scanning microscopy imaging. Water Sci. Technol. **47**(5)**:**31–37.
78. **McLean JS, Ona ON, Majors PD.** 2008. Correlated biofilm imaging,

transport and metabolism measurements via combined nuclear magnetic resonance and confocal microscopy. ISME J. **2:**121–131.
79. **Xavier JB, Picioreanu C, van Loosdrecht MCM.** 2004. Assessment of three-dimensional biofilm models through direct comparison with confocal microscopy imaging. Water Sci. Technol. **49**(11-12):177–185.
80. **Wagner M, Ivleva NP, Haisch C, Niessner R, Horn H.** 2009. Combined use of confocal laser scanning microscopy (CLSM) and Raman microscopy (RM): investigations on EPS-matrix. Water Res. **43:**63–76.
81. **Burnat M, Diestra E, Esteve I, Solé A.** 2009. *In situ* determination of the effects of lead and copper on cyanobacterial populations in microcosms. PLoS One **4:**e6204. doi:10.1371/journal.pone.0006204.
82. **Fortin D, Langley S.** 2005. Formation and occurrence of biogenic iron-rich minerals. Earth Sci. Rev. **72:**1–19.
83. **Hohmann C, Morin G, Ona-Nguema G, Guigner J-M, Brown GE, Jr, Kappler A.** 2011. Molecular-level modes of As binding to Fe(III) (oxyhydr)oxides precipitated by the anaerobic nitrate-reducing Fe(II)-oxidizing *Acidovorax* sp. strain BoFeN1. Geochim. Cosmochim. Acta **75:**4699–4712.
84. **Miot J, Benzerara K, Obst M, Kappler A, Hegler F, Schaedler S, Bouchez C, Guyot F, Morin G.** 2009. Extracellular iron biomineralization by photoautotrophic iron-oxidizing bacteria. Appl. Environ. Microbiol. **75:**5586–5591.
85. **Kumar M, Kumar N, Bhalla V.** 2011. FRET-induced nanomolar detection of Fe^{2+} based on cinnamaldehyde-rhodamine derivative. Tetrahedron Lett. **52:**4333–4336.
86. **Li P, Fang L, Zhou H, Zhang W, Wang X, Li N, Zhong H, Tang B.** 2011. A new ratiometric fluorescent probe for detection of Fe^{2+} with high sensitivity and its intracellular imaging applications. Chemistry **17:**10520–10523.
87. **Mei QS, Jiang CL, Guan GJ, Zhang K, Liu BH, Liu RY, Zhang ZP.** 2012. Fluorescent graphene oxide logic gates for discrimination of iron (3+) and iron (2+) in living cells by imaging. Chem. Commun. **48:**7468–7470.
88. **Bae S, Tae J.** 2007. Rhodamine-hydroxamate-based fluorescent chemosensor for Fe^{III}. Tetrahedron Lett. **48:**5389–5392.
89. **Dong L, Wu C, Zeng X, Mu L, Xue S-F, Tao Z, Zhang J-X.** 2010. The synthesis of a rhodamine B Schiff-base chemosensor and recognition properties for Fe^{3+} in neutral ethanol aqueous solution. Sens. Actuators B Chem. **145:**433–437.
90. **She M, Yang Z, Yin B, Zhang J, Gu J, Yin W, Li J, Zhao G, Shi Z.** 2012. A novel rhodamine-based fluorescent and colorimetric "off-on" chemosensor and investigation of the recognizing behavior towards Fe^{3+}. Dyes Pigments **92:**1337–1343.
91. **Zhang L-F, Zhao J-L, Zeng X, Mu L, Jiang X-K, Deng M, Zhang J-X, Wei G.** 2011. Tuning with pH: the selectivity of a new rhodamine B derivative chemosensor for Fe^{3+} and Cu^{2+}. Sens. Actuators B Chem. **160:**662–669.
92. **Huang L, Hou FP, Xi P, Bai D, Xu M, Li Z, Xie G, Shi Y, Liu H, Zeng Z.** 2011. A rhodamine-based "turn-on" fluorescent chemodosimeter for Cu^{2+} and its application in living cell imaging. J. Inorg. Biochem. **105:**800–805.
93. **Yu F, Zhang W, Li P, Xing Y, Tong L, Ma J, Tang B.** 2009. Cu^{2+}-selective naked-eye and fluorescent probe: its crystal structure and application in bioimaging. Analyst **134:**1826–1833.
94. **Zhu H, Fan J, Lu J, Hu M, Cao J, Wang J, Li H, Liu X, Peng X.** 2012. Optical Cu^{2+} probe bearing an 8-hydroxyquinoline subunit: high sensitivity and large fluorescence enhancement. Talanta **93:**55–61.
95. **Du P, Lippard SJ.** 2010. A highly selective turn-on colorimetric, red fluorescent sensor for detecting mobile zinc in living cells. Inorg. Chem. **49:**10753–10755.
96. **Min G, Lü-Bing T, Li J, Jian S, Gui Y.** 2009. A highly sensitive and selective colorimetric fluorescent zinc sensor based on fluorescein. Chin. J. Inorg. Chem. **25:**956–961.
97. **Xu L, Xu Y, Zhu W, Zeng B, Yang C, Wu B, Qian X.** 2011. Versatile trifunctional chemosensor of rhodamine derivative for Zn^{2+}, Cu^{2+} and His/Cys in aqueous solution and living cells. Org. Biomol. Chem. **9:**8284–8287.
98. **Childress ES, Roberts CA, Sherwood DY, LeGuyader CLM, Harbron EJ.** 2012. Ratiometric fluorescence detection of mercury ions in water by conjugated polymer nanoparticles. Anal. Chem. **84:**1235–1239.
99. **Liu Y, Lv X, Zhao Y, Chen M, Liu J, Wang P, Guo W.** 2012. A naphthalimide-rhodamine ratiometric fluorescent probe for Hg^{2+} based on fluorescence resonance energy transfer. Dyes Pigments **92:**909–915.
100. **Wang L, Zheng B, Zhao Y, Du J, Xiao D.** 2012. A Hg^{2+} selective fluorescent chemosensor based on rhodamine B thiohydrazide and its application in bioimaging. Anal. Methods **4:**2369–2374.

Likai Hao is a Ph.D. student in the Emmy-Noether junior research group "Environmental Analytical Microscopy" at the Eberhard Karls University of Tuebingen. His interest in microscopy was sparked as a master student of Prof. Xiangmei Liu in the State Key Laboratory of Microbial Technology of Shandong University and as an atomic force/probe scanning microscopy engineer under Prof. Nianzhi Jiao in the State Key Laboratory of Marine Environmental Science of Xiamen University. Here, he applied his microscopy experience to questions in microbial molecular biology and marine microbial ecology. After 4 years of working, he joined the Environmental Analytical Microscopy group, where he is developing fluorescent-probe-based quantitative confocal laser scanning microscopy approaches to study the fate of heavy metals in the environment.

Jianli Li was born in 1973. He received his B.Sc. degree in organic chemistry in 1997 from the Northwest University and his Ph.D. degree in organic chemistry at the same university under the supervision of Professor Zhi Shi in 2007. From 2007 to 2011, he performed a postdoc at the College of Life Sciences of the Northwest University on the synthesis and applications of photosensitive fluorescent probes. He joined the College of Chemistry and Materials Science of the Northwest University in 1997 where he is now a Professor. His scientific interests are firmly based in the areas of synthesis and research methods for organic substance, fluorescent molecular devices, chemical and biological sensors, and molecular recognition. He visited the University of Strasbourg, for 3 months, in 2012.

Continued next page

Andreas Kappler has held his current position as Professor of Geomicrobiology at Eberhard Karls University of Tuebingen since 2008. He received his diploma in chemistry and his Ph.D. in environmental microbiology and microbial ecology at the University of Konstanz in Germany in 2000. After a postdoc at EAWAG/ETH in Zürich in environmental chemistry and a postdoc at Caltech in geobiology, he moved to Tübingen in 2004 to head an Emmy-Noether junior research group in geomicrobiology before being appointed Professor of Geomicrobiology. His research focuses on the formation and transformation of iron minerals by Fe(II)-oxidizing and Fe(III)-reducing bacteria and the implications of these processes for the fate of pollutants in soils and sediments as well as for the deposition of iron minerals on early Earth. His research combines microbial cultivation, molecular biology, fluorescence and electron microscopy, Mössbauer spectroscopy, and synchrotron-based X-ray absorption spectroscopy and spectromicroscopy.

Martin Obst is the head of the Emmy-Noether junior research group "Environmental Analytical Microscopy" at the Eberhard Karls University of Tuebingen. He received his Ph.D. in geomicrobiology in the group of Prof. Bernhard Wehrli from the Swiss Federal Institute of Technology, Zurich, Switzerland/Swiss Federal Institute of Aquatic Science and Technology, Kastanienbaum, Switzerland. During his Ph.D., he gained expertise in electron and atomic force microscopy. He followed up this experience with a 2.5-year postdoctoral fellowship at the scanning transmission X-ray microscopy beamline at the Canadian Light Source. His current research interests are using analytical microscopy to study the distribution, mobility, and bioavailability of toxic trace metals and other contaminants in the environment.